ISSN 2176-5480

22nd International Congress of Mechanical Engineering (COBEM 2013)
November 3-7, 2013, Ribeirão Preto, SP, Brazil

A COMPARISON OF TWO INVERSE PROBLEM TECHNIQUES FOR THE IDENTIFICATION OF CONTACT FAILURES IN MULTI-LAYERED COMPOSITES

Luiz Alberto da Silva Abreu
Marcelo José Colaço
Federal University of Rio de Janeiro, PEM-COPPE-UFRJ, Cx. Postal 68503, Rio de Janeiro, RJ, 21941-972, Brazil
luizabreu@ufrj.br, colaco@ufrj.br

Carlos José Santos Alves
Technical University of Lisbon, Av. Rovisco Pais, 1, Lisbon, 1049-001, Portugal
carlos.alves@math.ist.utl.pt

Helcio Rangel Barreto Orlande
Federal University of Rio de Janeiro, PEM-COPPE-UFRJ, Cx. Postal 68503, Rio de Janeiro, RJ, 21941-972, Brazil
helcio@mecanica.coppe.ufrj.br

Ville Kolehmainen
Department of Applied Physics, University of Eastern Finland, P.O. Box 1627, 70211, Kuopio, Finland
ville.kolehmainen@uef.fi

Jari Kaipio
Department of Mathematics, University of Auckland, PB 92019, Auckland Mail Centre, Auckland 1142, New Zealand
jari@math.auckland.ac.nz

Abstract. *This paper deals with the solution of an inverse heat conduction problem of identifying the interface thermal contact conductance between layers of multi-layered composite materials. Two techniques are used and compared for the solution of the inverse problem. One of these techniques is formulated in terms of a reciprocity functional approach, together with the method of fundamental solutions. This solution is composed of two steps. In the first step, two steady-state auxiliary problems, which do not depend on the thermal conductance variation, are solved. With the results of this pre-processing, different thermal conductances can be recovered by simply performing an integration. The other technique examined in this work is the Markov chain Monte Carlo (MCMC) method, within the Bayesian framework. A total variation prior is used for the spatially distributed contact conductance for the MCMC method. The solution of the inverse problem is evaluated with simulated temperature measurements, supposedly taken with large spatial resolution and large frequency, by using an infrared camera.*

Keywords: *thermal contact resistance, reciprocity functional, Bayesian approach*

1. INTRODUCTION

Thermal contact conductance is very important in many heat transfer applications, such as electronic packaging (Zhang et al, 2004), nuclear reactors (Milosevic et al, 2002), aerospace and biomedicine (McWaid and Marschall, 1992), among others. It has been recognized for several years (Edmonds et al, 1978) that the increasing power density of some electronic equipment requires cooling devices able to remove great amounts of heat. In fact, there is an interest in producing microchannel heat sinks with heat removal capacities of more than 1 KW/cm^2 (Jiang et al, 2001). An important factor in obtaining such heat removal is to have a low thermal contact resistance between the electronics and the cooling devices. In nuclear reactors, resistance, which occurs in the gap between the nuclear fuel and the metallic cladding, has become a limiting factor in exploiting reactor efficacy (Milosevic et al, 2002).

When two materials are in contact, only fractions of them are really touching each other. Thus, there is a discontinuity in the temperature across the contact interface. Thermal contact resistance is defined as the ratio of the temperature drop to the heat flow rate across the interface.

$$R_c = \Delta T / q \tag{1}$$

ISSN 2176-5480

Thus, lower values of R_c indicate that the difference in the temperature across the interface is low, which demonstrates a good contact. Thermal contact conductance, in the context of this paper, is defined as the inverse of the resistance (h=1/R_c). Notice that both R_c and h can vary spatially along the interface. Some studies (Halliday et al, 1996; Zhang et al, 2004; Liu et al, 2010; Luo et al, 2011) used the definition given by Eq. (1) to calculate the global thermal contact resistance of several materials. These studies, in general, used an experimental apparatus to measure the discontinuity in temperature and the heat flux applied. Because the discontinuity at the exact location of the interface is difficult to measure, they took temperature measurements at several locations and extrapolated the value of the temperature at the interface. Wolff and Schneider (1998) used the guarded hot plate method to determine temperature discontinuities across interfaces. The disadvantage of such methods is that they only predict global values of the thermal contact resistance/conductance. In addition, they require complicated experimental apparatus and/or some intrusive temperature measurements.

Milosevic et al. (2002) used a non-intrusive method, the laser flash method, together with the Gauss method to estimate a constant value of the thermal contact resistance between two solids. In their paper, they were able to estimate this parameter when the sample materials were good heat conductors or when the thickness of the layer was relatively small. In addition, the accuracy of the estimate increased with higher values of the contact resistance. Thus, voids with very small values of the thermal contact resistance could not be very well captured. Milosevic also presented other results (2003) using the laser flash method.

Fieberg and Kneer (2007) solved an inverse heat conduction problem to estimate the heat flux at the interface between two solids and used temperature measurements at the interface to estimate the thermal contact resistance. In their work, the measurements were taken by an infrared camera pointed at the location of the interface. Thus, they needed access to the location of the interface. In addition, a time dependent global contact resistance with constant spatial distribution was estimated because no interior evaluation of the interface was performed. Yang (2007) also used an inverse heat conduction problem to estimate a time dependent contact resistance in single-coated optical fibers. Although good results were obtained, intrusive measurements were required. No spatial variation was considered.

Gill et al. (2009) solved an inverse heat conduction problem to estimate the spatial distribution of the thermal contact resistance. The authors mentioned that several models (as cited above) consider the resistance constant, although it actually varies spatially. The results obtained by the authors were very sensitive to measurement errors and required the use of a regularization technique. In addition, the temperatures were measured very close to the interface, making the method very intrusive. However, the main contribution was to estimate the spatial variation of the thermal contact resistance instead of using a constant value.

Abreu et al (2011) formulated an inverse problem, within the Bayesian framework with a Markov Chain Monte Carlo method to identify thermal contact resistances in multilayered materials, using non-intrusive measurements, through the readings of an infrared camera. The direct problem was solved with a hybrid approach, based on the Generalized Integral Transform Technique and finite-differences. Results obtained with simulated measurements revealed the capabilities of such approach, mainly when non-informative prior models were used in the solution of the inverse problem. In fact, the regions of contact failures and perfect contact were accurately identified by this approach.

Colaço and Alves (2013) presented a method to estimate thermal contact conductance in steady-state problems without intrusive measurements. The methodology presented was formulated in terms of a reciprocity functional approach (Andrieux and Abda, 1993) together with the method of fundamental solutions (Kupradze and Aleksidze, 1963) to solve two auxiliary problems. The solution was composed of two steps. In the first step, auxiliary problems, which did not depend on the thermal conductance variation, were solved. With the results of pre-processing, different thermal conductances could be recovered by simply performing an integral. Thus, the methodology was extremely fast and could be used to detect flaws in different species using a short computational time.

According to the discussion above, the determination of the thermal contact resistance/conductance is a very difficult task. The objective of this paper is to compare two different methodologies to estimate the spatial variation of this parameter without intrusive measurements. The method proposed by Colaço and Alves (2013) and the Bayesian framework with a Markov Chain Monte Carlo method applied by Abreu et al (2011) will be compared in terms of accuracy.

2. PHYSICAL PROBLEM

Let us consider a generic domain Ω, divided in three parts $\Omega = \Omega_1 \cup \Gamma \cup \Omega_2$, where Ω_1 is the first domain, with a thermal conductivity K_1, Ω_2 is the second domain, with a thermal conductivity K_2, and Γ is the contact surface between them. The boundary of Ω_1 is $\partial\Omega_1 = \Gamma_o \cup \Gamma_1 \cup \Gamma$, where the surface Γ_o is subjected to a prescribed heat flux and its temperature is measured. Γ_1 is the lateral surface of Ω_1, and Γ is the contact surface between Ω_1 and Ω_2. On the other hand, the boundary of Ω_2 is $\partial\Omega_2 = \Gamma_{oo} \cup \Gamma_2 \cup \Gamma$, where Γ_{oo} is the lower surface, Γ_2 is the lateral surface of Ω_2 and Γ is the contact surface. Fig. 1 shows the geometry for a two-dimensional case.

ISSN 2176-5480

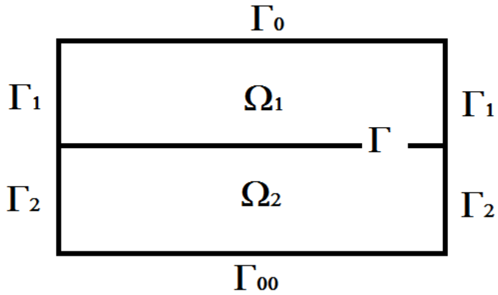

Figure 1. Geometry for a two-dimensional case

The lateral surfaces Γ_1 U Γ_2 are assumed to be thermally insulated while the lower surface Γ_{oo} is subjected to a prescribed temperature. The measurement surface Γ_o is assumed to have a prescribed heat flux q imposed on it. The contact surface Γ is assumed to have a Robin boundary condition, i.e., $-K_1\partial_{\mathbf{n}}T_1 = h(T_1 - T_2)$, where **n** is the normal derivative outward the boundary, K_1 is the thermal conductivity of region 1, T_1 and T_2 are the temperatures at the interface of domains one and two, respectively, and h is the thermal contact conductance, which varies from zero (for total contact failure) to infinity (for perfect contact). Actually, in practice, large values of h are already sufficient to characterize a perfect contact, when the temperature drop across the interface becomes negligible.

The statement of the interface heat transfer problem in the steady-state case for constant conductivities K_1 and K_2 can be formulated as the following *direct problem*:

$$\nabla^2 T_1 = 0 \quad \text{in } \Omega_1 \tag{2.a}$$

$$-K_1 \frac{\partial T_1}{\partial \mathbf{n}} = q \quad \text{at } \Gamma_o \tag{2.b}$$

$$\frac{\partial T_1}{\partial \mathbf{n}} = 0 \quad \text{at } \Gamma_1 \tag{2.c}$$

$$-K_1 \frac{\partial T_1}{\partial \mathbf{n}} = h(T_1 - T_2) \quad \text{at } \Gamma \tag{2.d}$$

$$\nabla^2 T_2 = 0 \quad \text{in } \Omega_2 \tag{2.e}$$

$$\frac{\partial T_2}{\partial \mathbf{n}} = 0 \quad \text{at } \Gamma_2 \tag{2.f}$$

$$T_2 = 0 \quad \text{at } \Gamma_{oo} \tag{2.g}$$

$$K_2 \frac{\partial T_2}{\partial \mathbf{n}} = -K_1 \frac{\partial T_1}{\partial \mathbf{n}} \quad \text{at } \Gamma \tag{2.h}$$

The *inverse problem* consists of estimating the function h at the inaccessible contact surface Γ by using temperature measurements Y at the boundary Γ_o. These measurements can be accurately taken with nowadays available infrared cameras, which can provide experimental data with high spatial resolutions and high frequencies.

3. RECIPROCITY FUNCTIONAL APPROACH

The reciprocity functional approach to identify the unknown function h (Colaço and Alves, 2013) is composed of two steps: in the first one, the temperature difference T_1-T_2 at the inaccessible boundary Γ is obtained by a first auxiliary problem and in the second step the heat flux is obtained at this same boundary, using a second auxiliary problem. At the end, both results are combined to obtain the thermal contact conductance. Indeed, according to Eq. (2.d), the thermal contact conductance will be given as the ratio of these two quantities. Note that if (T_1-T_2) is equal to zero, then we have a perfect thermal contact between both surfaces and the definition of thermal contact resistance does not make sense (h tends to infinity).

3.1 Obtaining T_1-T_2 at Γ

Consider the *first auxiliary problem* for some harmonic test functions $F_1 \in C^2(\Omega_1)$ and $F_2 \in C^2(\Omega_2)$:

$$\nabla^2 F_1 = 0 \quad \text{in } \Omega_1 \tag{3.a}$$

$$K_1 \frac{\partial F_1}{\partial \mathbf{n}} = \varphi \quad \text{at } \Gamma \tag{3.b}$$

$$\frac{\partial F_1}{\partial \mathbf{n}} = 0 \quad \text{at } \Gamma_1 \tag{3.c}$$

$$F_1 = F_2 \quad \text{at } \Gamma \tag{3.d}$$

$$\nabla^2 F_2 = 0 \quad \text{in } \Omega_2 \tag{3.e}$$

$$\frac{\partial F_2}{\partial \mathbf{n}} = 0 \quad \text{at } \Gamma_2 \tag{3.f}$$

$$F_2 = 0 \quad \text{at } \Gamma_{oo} \tag{3.g}$$

$$K_2 \frac{\partial F_2}{\partial \mathbf{n}} = -K_1 \frac{\partial F_1}{\partial \mathbf{n}} \quad \text{at } \Gamma \tag{3.h}$$

The F_1 problem is a Cauchy Problem. Thus, there are two boundary conditions at the same surface Γ and there is no boundary condition for F_1 at Γ_0. For the F_2 problem, that is a Laplace Problem, there is one boundary condition for each surface of Ω_2 domain. Note that φ appearing in Eq. (3.b) is a generic basis function, which will be defined later.

Let us write the following identity for the domain Ω_1:

$$0 = \int_{\Omega_1} \left[F_1 \left(\nabla^2 T_1 \right) - T_1 \left(\nabla^2 F_1 \right) \right] d\Omega_1 \tag{4}$$

Using Eqs. (2.a) and (3.a), both Laplacians are zero such that Eq. (4) vanishes. By using Green´s second identity, we can, however, obtain

$$\begin{aligned} \int_{\Omega_1} \left[F_1 \left(\nabla^2 T_1 \right) - T_1 \left(\nabla^2 F_1 \right) \right] d\Omega_1 &= \int_{\partial\Omega_1} \left[F_1 \frac{\partial T_1}{\partial \mathbf{n}} - T_1 \frac{\partial F_1}{\partial \mathbf{n}} \right] d\left(\partial\Omega_1\right) \\ 0 &= \int_{\Gamma_0 \cup \Gamma_1 \cup \Gamma} \left[F_1 \frac{\partial T_1}{\partial \mathbf{n}} - T_1 \frac{\partial F_1}{\partial \mathbf{n}} \right] d\left(\partial\Omega_1\right) \end{aligned} \tag{5}$$

After some manipulations (Colaço and Alves, 2013), and using the boundary conditions on Γ_1, Eqs. (2.c) and (3.c), together with Eq. (2.b) and the fact the some measurements Y are available at the boundary Γ_0, such that $T_1=Y$ at Γ_0, we obtain

$$0 = \int_{\Gamma_0} \left[F_1 \left(\frac{-q}{K_1} \right) - Y \frac{\partial F_1}{\partial \mathbf{n}} \right] d\Gamma_0 + \int_{\Gamma} \left[F_1 \frac{\partial T_1}{\partial \mathbf{n}} - T_1 \frac{\partial F_1}{\partial \mathbf{n}} \right] d\Gamma \tag{6}$$

Let us now consider another identity, for the domain Ω_2:

$$0 = \int_{\Omega_2} \left[F_2 \left(\nabla^2 T_2 \right) - T_2 \left(\nabla^2 F_2 \right) \right] d\Omega_2 \tag{7}$$

where the Laplacians are taken from Eqs. (2.e) and (3.e) such that Eq. (7) vanishes. By using Green´s second identity, as well as Eqs. (2.f), (2.g), (3.f) and (3.g), we can obtain

$$0 = \int_{\Gamma} \left[F_2 \frac{\partial T_2}{\partial \mathbf{n}} - T_2 \frac{\partial F_2}{\partial \mathbf{n}} \right] d\Gamma \tag{8}$$

As K_1 and K_2 are constants, summing Eqs. (6) and (8), and using Eqs. (2.h), (3.d), and (3.h), we finally obtain

$$\int_{\Gamma_0} K_1 \left[F_1 \left(\frac{-q}{K_1} \right) - Y \frac{\partial F_1}{\partial \mathbf{n}} \right] d\Gamma_0 = \int_{\Gamma} K_1 \frac{\partial F_1}{\partial \mathbf{n}} \left[T_1 - T_2 \right] d\Gamma \tag{9}$$

Now we can define $\mathcal{R}(F_1)$ as the reciprocity functional, a notion used by Andrieux and Ben Abda (1993), in terms of the test functions F_1 as

$$\mathcal{R}(F_1) = \int_{\Gamma_o} \left[F_1 \left(\frac{-q}{K_1} \right) - Y \frac{\partial F_1}{\partial \mathbf{n}} \right] d\Gamma_o \tag{10}$$

For the calculation of the reciprocity functional, no information regarding the boundary Γ is needed. In addition, once the function F_1 is specified, only the conductivity K_1, the imposed heat flux q and the measured temperature Y are needed for the calculation of $\mathcal{R}(F_1)$. Using Eqs. (9) and (10), we obtain

$$\mathcal{R}(F_1) K_1 = \left\langle T_1 - T_2, K_1 \frac{\partial F_1}{\partial \mathbf{n}} \right\rangle_{L^2(\Gamma)} \tag{11}$$

Now take $F_{1,j}$ such that $K_1 \partial_{\mathbf{n}} F_{1,j} = \varphi_j$ at Γ [Eq.(3.b)], where (φ_j) is a $L^2(\Gamma)$ orthonormal basis system. Then, taking the projection of Eq. (11) over φ_j, the discontinuity T_1-T_2 can be written as

$$\left[T_1 - T_2 \right]_{\Gamma} = \sum_j \left\langle T_1 - T_2, \varphi_j \right\rangle_{L^2(\Gamma)} \varphi_j = \sum_j \mathcal{R}\left(F_{1,j} \right) K_1 \varphi_j \tag{12}$$

To obtain the functions $F_{1,j}$, we must solve a Cauchy problem with double conditions $K_1 \partial_{\mathbf{n}} F_{1,j} = \varphi_j$ and $F_{1,j} = F_{2,j}$ at the boundary Γ. The problem has to be solved thus for several functions φ_j. The solution of the auxiliary problem is *independent* of the direct problem, except by the geometry and the thermal conductivity K_1. Thus, once the auxiliary problem is solved and the functions $F_{1,j}$ are obtained, different discontinuity configurations T_1-T_2 can be obtained by simply evaluating a different integral in Eq. (10). Equation (12) also allows to identify situations of perfect thermal contact (T_1=T_2) where we can avoid the division in the definition of h.

3.2 Obtaining -$K_1 \partial_{\mathbf{n}} T_1$ at Γ

Consider now the *second auxiliary problem*, for some harmonic test functions $G_1 \in C^2(\Omega_1)$:

$\nabla^2 G_1 = 0$	in Ω_1	(13.a)
$G_1 = \varphi$	at Γ	(13.b)
$\frac{\partial G_1}{\partial \mathbf{n}} = 0$	at Γ_1	(13.c)
$\frac{\partial G_1}{\partial \mathbf{n}} = 0$	at Γ	(13.d)

Following the same procedure used in section 3.1, we can obtain (Colaço and Alves, 2013):

$$-\left[K_1 \frac{\partial T_1}{\partial \mathbf{n}} \right]_{\Gamma} = -\sum_j \left\langle K_1 \frac{\partial T_1}{\partial \mathbf{n}}, \varphi_j \right\rangle_{L^2(\Gamma)} \varphi_j = \sum_j \mathcal{R}\left(G_{1,j} \right) K_1 \varphi_j \tag{14}$$

where

$$\mathcal{R}(G_1) = \int_{\Gamma_0} \left[G_1 \left(-\frac{q}{K_1} \right) - Y \frac{\partial G_1}{\partial \mathbf{n}} \right] d\Gamma_o \tag{15}$$

ISSN 2176-5480

To find the functions $G_{1,j}$, we must solve a Cauchy problem with double conditions $G_{1,j}=\varphi_j$ and $\partial_{\mathbf{n}}G_{1,j}=0$ at the boundary Γ. Once again, the solution of the auxiliary problem is ***independent*** of the direct problem, except in terms of the geometry, which is the same. Thus, once the auxiliary problem is solved and the functions $G_{1,j}$ are obtained, different heat fluxes $-K_1\partial_{\mathbf{n}}T_1$ can be obtained by simply evaluating a different integral in Eq. (15), which is the main advantage of this method because the pre-processing involved in solving the auxiliary problems is performed only once. Then, different thermal contact conductances can be recovered by simply solving different integrals.

3.3 **Obtaining** *h*

From the previous results, the value of h can be obtained as

$$h = \frac{\sum_j \mathcal{R}\left(G_{1,j}\right)\varphi_j}{\sum_j \mathcal{R}\left(F_{1,j}\right)\varphi_j} \tag{16}$$

It is worthwhile to mention that the two Cauchy problems were solved by the Method of Fundamental Solutions. More details can be found in Colaço and Alves (2013).

4. MARKOV CHAIN MONTE CARLO METHOD APPROACH

The MCMC method used in this work was applied to a three-dimensional version of the problem presented in Fig. 1, which is presented in Fig. 2. In order to make the problem close to the one presented in Fig. 1, and thus make possible the comparison of both methods, h_{∞} was set to a very large value (to ensure a constant temperature at the bottom surface of the material), $h_{\circ}$ to a very small value (to ensure a constant heat flux applied at the top surface) and the walls perpendicular to the *y*-axis were set thermally insulated. Also, the imposed heat flux was supposed to be steady and vary only in the *x* direction. Such problem was solved by the Generalized Integral Transform Technique. More details can be found in Abreu et al (2011).

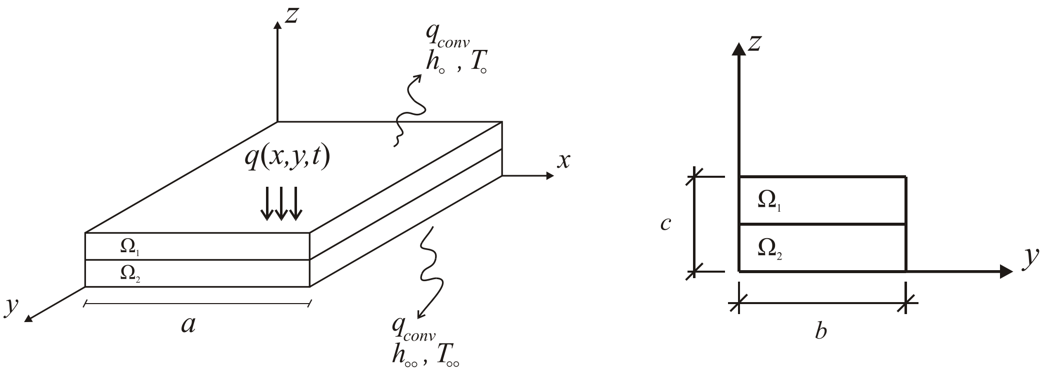

Figure 2. Geometry for a three-dimensional case

For the MCMC solution of this problem, consider that the vector containing the measured temperatures is written as:

$$\mathbf{Y}^T = \left(\vec{Y}_1, \vec{Y}_2, \ldots, \vec{Y}_{k_{\max}}\right) \tag{17.a}$$

where $\vec{Y}_k$ contains the measured temperatures of *M* sensors (pixels of the infrared camera) at time t_k, $k = 1, \ldots, k_{\max}$, that is,

$$\vec{Y}_k = (Y_{k1}, Y_{k2}, \ldots, Y_{kM}) \qquad \text{for } k = 1, \ldots, k_{\max} \tag{17.b}$$

so that we have $D = Mk_{max}$ measurements in total.

The contact conductance *h* is assumed to be uniform within the elements of a grid analogous to that provided by the spatial resolution of the infrared camera. Hence, the unknowns to be estimated can be written in the form of a vector of parameters

$$\mathbf{P}^T = \left[h_1, h_2, \ldots, h_M\right] \tag{18}$$

ISSN 2176-5480

Such parameters are estimated with a technique within the Bayesian framework. In this case, the solution of the inverse problem is recast in the form of statistical inference from the *posterior probability density*, which is the model for the conditional probability distribution of the unknown parameters given the measurements. The measurement model incorporating the related uncertainties is called the *likelihood*, that is, the conditional probability of the measurements given the unknown parameters. The model for the unknowns that reflects all the uncertainty of the parameters without the information conveyed by the measurements, is called the *prior* model [7,9].

The formal mechanism to combine the new information (measurements) with the previously available information (prior) is known as the Bayes' theorem (Kaipio and Somersalo, 2004; Tan et al, 2006). Therefore, the term Bayesian is often used to describe the statistical inversion approach, which is based on the following principles (Kaipio and Somersalo, 2004): 1. All variables included in the model are modeled as random variables; 2. The randomness describes the degree of information concerning their realizations; 3. The degree of information concerning these values is coded in probability distributions; and 4. The solution of the inverse problem is the posterior probability distribution, from which distribution point estimates and other statistics are computed. On the other hand, classical regularization methods are not based on the modeling of prior information and related uncertainties about the unknown parameters.

Bayes' theorem is stated as (Kaipio and Somersalo, 2004; Tan et al, 2006):

$$\pi_{posterior}(\mathbf{P}) = \pi(\mathbf{P}|\mathbf{Y}) = \frac{\pi(\mathbf{P})\pi(\mathbf{Y}|\mathbf{P})}{\pi(\mathbf{Y})} \tag{19}$$

where $\pi_{posterior}(\mathbf{P})$ is the posterior probability density, $\pi(\mathbf{P})$ is the prior density, $\pi(\mathbf{Y}|\mathbf{P})$ is the likelihood function and $\pi(\mathbf{Y})$ is the marginal probability density of the measurements, which plays the role of a normalizing constant.

By assuming that the measurement errors are Gaussian random variables, with zero means and known covariance matrix $\mathbf{W}$ and that the measurement errors are additive and independent of the parameters $\mathbf{P}$, the *likelihood function* can be expressed as (Kaipio and Somersalo, 2004; Tan et al, 2006):

$$\pi(\mathbf{Y}|\mathbf{P}) = (2\pi)^{-D/2}\left|\mathbf{W}\right|^{-1/2}\exp\left\{-\frac{1}{2}\left[\mathbf{Y}-\mathbf{T}(\mathbf{P})\right]^T\mathbf{W}^{-1}\left[\mathbf{Y}-\mathbf{T}(\mathbf{P})\right]\right\} \tag{20}$$

where $\mathbf{T}(\mathbf{P})$ is the solution of the direct (forward) problem, with known vector $\mathbf{P}$ given by Eq. (18)..

A total variation non-informative prior is used in this work for the spatially distributed contact conductance. Such a prior density is a Markov random field, capable of accurately discriminating regions with uniform values of the sought distributed function (Kaipio and Somersalo, 2004). Therefore, the posterior distribution is given by:

$$\pi(\mathbf{P}|\mathbf{Y}) \propto \exp\left\{-\frac{1}{2}[\mathbf{Y}-\mathbf{T}(\mathbf{P})]^T\mathbf{W}^{-1}[\mathbf{Y}-\mathbf{T}(\mathbf{P})] - \gamma\, TV(\mathbf{P})\right\} \tag{21}$$

where $\gamma > 0$ controls the smoothness of the inverse problem solution.

Estimates from the posterior distribution typically require numerical integration. In these cases, sampling based on Markov chain Monte Carlo (MCMC) methods is the most feasible technique for the computation of the estimates, especially in cases where the number of unknowns is not too large (Kaipio and Somersalo, 2004).

The most common MCMC algorithm is the Metropolis-Hastings algorithm (Kaipio and Somersalo, 2004; Tan et al, 2006). The implementation of the Metropolis-Hastings algorithm starts with the selection of a proposal distribution $p(\mathbf{P}^*,\mathbf{P}^{(t-1)})$ which is used to draw a new candidate state $\mathbf{P}^*$, given the current state $\mathbf{P}^{(t-1)}$ of the Markov chain.

Once the jumping distribution has been selected, the Metropolis-Hastings sampling algorithm can be implemented by repeating the following steps:

1. Sample a *Candidate Point* $\mathbf{P}^*$ from a proposal distribution $p(\mathbf{P}^*,\mathbf{P}^{(t-1)})$.
2. Calculate the acceptance factor:

$$\alpha = \min\left\{1, \frac{\pi\left(\mathbf{P}^* \mid \mathbf{Y}\right)p\left(\mathbf{P}^*,\mathbf{P}^{(t-1)}\right)}{\pi\left(\mathbf{P}^{(t-1)} \mid \mathbf{Y}\right)p\left(\mathbf{P}^{(t-1)},\mathbf{P}^*\right)}\right\} \tag{22}$$

3. Generate a random value U which is uniformly distributed on (0,1).
4. If $U \leq \alpha$, set $\mathbf{P}^{(t)} = \mathbf{P}^*$. Otherwise, set $\mathbf{P}^{(t)} = \mathbf{P}^{(t-1)}$.
5. Return to step 1 in order to generate the sequence $\{\mathbf{P}^{(1)}, \mathbf{P}^{(2)}, \ldots, \mathbf{P}^{(n)}\}$.

We note that values of $\mathbf{P}^{(i)}$must be ignored while the chain has not converged to equilibrium (the burn-in period) (Kaipio and Somersalo, 2004; Tan et al, 2006). Despite the fact that all variables appearing in the mathematical formulation of the physical problem are generally modeled as random variables, within the Bayesian framework for the solution of inverse problems, in this work attention is focused on the estimation of only the contact conductance h. Therefore, the other parameters appearing in the formulation are taken into account in terms of their deterministic nominal values. Uncertainties on these judged known parameters can also be very conveniently considered in the inverse problem solution by using the novel approximation error approach (Nissinen et al, 2008, 2009, 2011; Orlande et al, 2013).

5. RESULTS

For the results presented below, the plate width and length were both taken as $a = b = 0.10$ m. The two layers were assumed to be of equal thickness (0.005 m), so that $c = 0.01$ m. Two test cases were considered, where the materials assumed for the layers were titanium ($k = 21.9$ W/mK and $\alpha = 9.32 \times 10^{-6}$ m^2/s), epoxy with graphite fibers - 25% vol ($k = 0.87$ W/mK and $\alpha = 0.66 \times 10^{-6}$ m^2/s), and AISI 1050 steel ($k = 54$W/mK and $\alpha = 1.474 \times 10^{-5}$ m^2/s). Table 1 shows the test cases analyzed.

Table 1. Test cases analyzed.

Test-case	Material for Ω_1	Material for Ω_2
1	titanium	epoxy with graphite fibers - 25%
2	AISI 1050 steel	AISI 1050 steel

In order to compare the two formulations, for the physical problems presented in Figs. 1 and 2, the heat transfer coefficients at the bottom and top surfaces of the plate represented in Fig. 2 were taken respectively as 10^{10} and 10^{-10} W/m^{2}K and a heat flux of 25,000 W/m^2 was imposed uniformly over the top surface. Thus, the 3D problem presented in Fig. 2 was transformed into the 2D problem presented in Fig. 1.

Simulated temperature measurements were used in this paper. Such measurements were generated by using the solution of the direct problem with a prescribed variation of the contact conductance h. The simulated measurements were obtained through the GITT solution of the problem presented in Fig. 2. Gaussian uncorrelated errors, with zero mean and constant standard deviation, were added to the solution of the direct problem. The grid at the heated surface, where the temperature measurements were considered available, involved $M = 441$ elements (21 in each of the x and y directions), which correspond to the pixels of the infrared camera. Consequently, the contact conductance h was estimated in a grid of same size for the MCMC method. The standard deviation of the measurement errors (σ) was of 0.01 ^{o}C and 0.1 ^{o}C. Since the solution of the reciprocity functional approach requires the integration of the measured temperature data at more points than the ones generated above, an interpolation procedure was used over these data, based on a cubic spline approximation.

The contact conductance h that was selected to generate the measurements aimed at simulating one region of total contact failure between the layers, with thermal contact in the remaining regions. The contact failure was simulated with $h = 0$ W/m^{2}K, while the contact was simulated with $h = 1044$ W/m^{2}K. Figs. 3 and 4 show the h profiles and the exact temperatures at two times for both test cases analyzed in this paper, where the largest time corresponds to steady-state conditions. In these figures it is also shown the maximum temperature difference for each time considered.

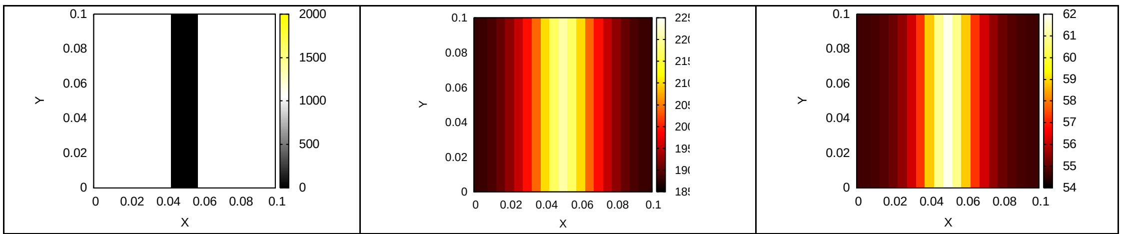

(a) Profile for the contact conductance | (b) Exact temperature (t=1000s), ΔT=40°C | (c) Exact temperature (t=30s), ΔT=8°C

Figure 3. Profile for the contact conductance and exact temperatures for test case 1.

ISSN 2176-5480

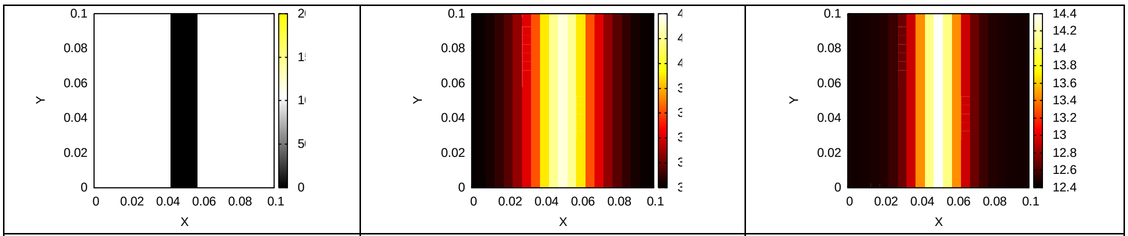

(a) Profile for the contact conductance | (b) Exact temperature (t=200s), ΔT=14°C | (c) Exact temperature (t=10s), ΔT=1.8°C

Figure 4. Profile for the contact conductance and exact temperatures for test case 2.

Figure 5 shows the recovered thermal contact conductance for test case 1, considering two levels of uncertainties. For this test case, where the bottom material has a very low thermal conductivity (0.87W/(mK)), the RF method presented a very unstable solution for the thermal contact conductance; whereas the MCMC method was able to reasonably well capture the contact discontinuity. In fact, the plot was cropped at 4000W/(m^{2}K), since the solution for the RF method close to the walls assumed a very large value. The MCMC method uses a 3D formulation and thus recovers a 2D function of the thermal contact conductance, while the RF method used in this paper recovers a 1D function. Thus, to make the comparison of the two methods on the same grounds, the solution for the MCMC method is presented for the function estimated along the X coordinate, for Y=0.05 m (see Figs. 3 and 4). Although this result can indicate a lack of accuracy for the RF method, if we look at the individual values captured for the temperature difference and heat flux at the contact interface, estimated by the RF method (see Fig. 6), a very good result can be found. In fact, since the main objective of this paper is to *detect* the contact failures and not to *quantify* the thermal contact conductance, results shown in Fig. 6 indicate that the RF method is capable of recovering the failure with accuracy comparable to that of the MCMC method (notice that the heat flux goes to zero at the failure, where the temperature difference reaches its maximum value).

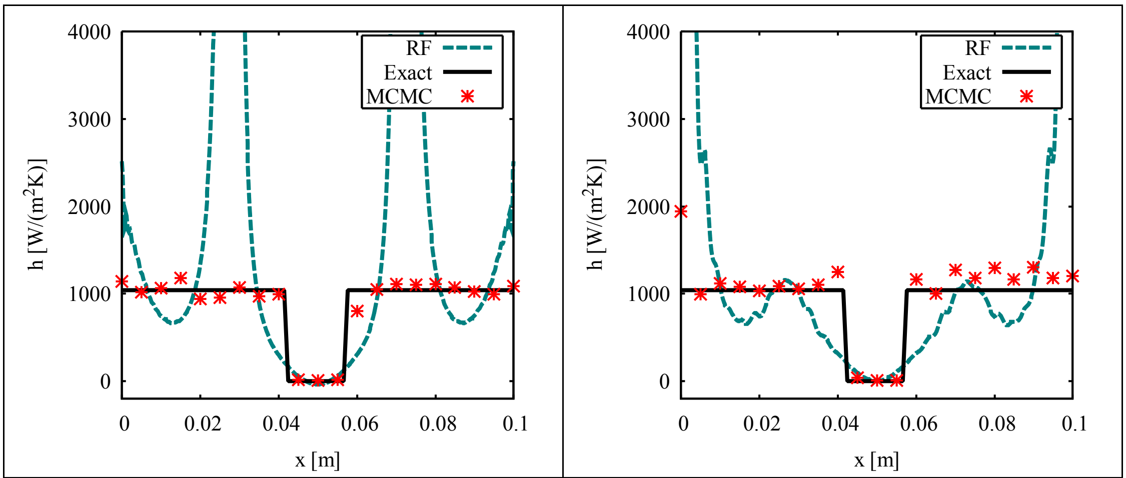

(a) σ =0.01 °C | (b) σ =0.1 °C

Figure 5. Recovered profile for the contact conductance for test case 1.

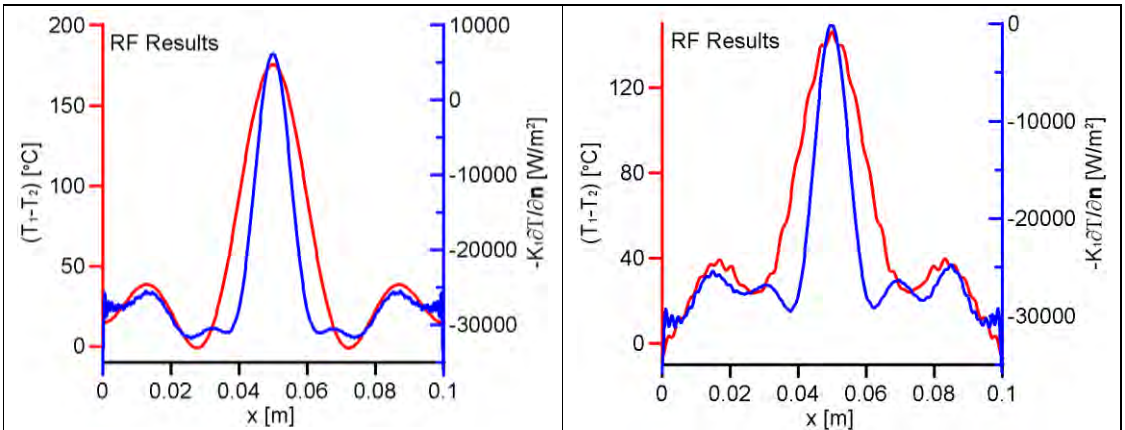

(a) σ =0.01 °C | (b) σ =0.1 °C

Figure 6. Recovered profile for the temperature difference and heat flux at the interface, for test case 1.

When we consider materials with higher thermal conductivities, such as the one used in test case 2, both the RF and the MCMC methods present estimates for the thermal contact conductance with comparable accuracy, as one can verify from Fig. 7.

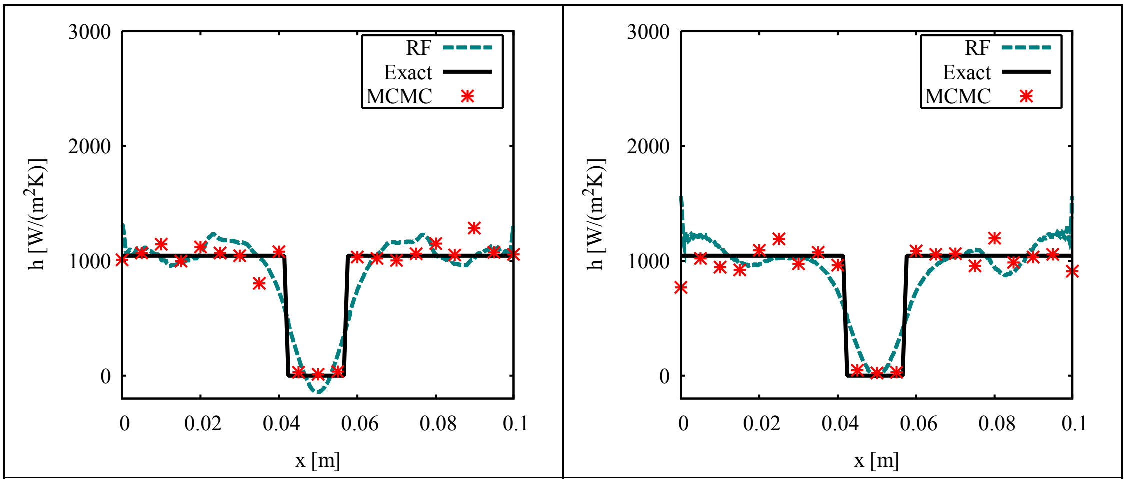

(a) σ =0.01 °C | (b) σ =0.1 °C

Figure 7. Recovered profile for the contact conductance for test case 2.

6. CONCLUSIONS

In this paper we applied two inverse problem techniques for the estimation of the thermal contact conductance in a double-layered material, by using surface temperature measurements. One of the techniques, the Reciprocity Functional Method, formulates the estimate as an integral of the measured data and thus, does not require any iterative process. The other technique, the Markov Chain Monte Carlo Method, is a Bayesian technique. For the test-cases examined here, both techniques are capable of accurately detecting the simulated contact failure.

7. ACKNOWLEDGEMENTS

The authors would like to thank the Brazilian agencies for the fostering of science, Conselho Nacional de Desenvolvimento Científico e Tecnológico (CNPq), Coordenação de Aperfeiçoamento de Pessoal de Nível Superior (CAPES), Fundação Carlos Chagas Filho de Amparo à Pesquisa do Estado do Rio de Janeiro (FAPERJ), and Programa de Recursos Humanos da Agência Nacional de Óleo, Gás Natural e Biocombustíveis (ANP/PRH) for the financial support for this work.

8. REFERENCES

Abreu, L. A., Orlande, H. R. B., Naveira-Cotta, C. P., Quaresma, J. N. N., Cotta, R. M., Kaipio, J., Kolehmainen, V., 2011, "Identification of Contact Failures in Multi-Layered Composites", *ASME 2011 International Design Engineering Technical Conference & Computers and Information Engineering Conference*, August 29-31, Washington, DC, US

Andrieux, S., and Abda, A.B., 1993, "The Reciprocity Gap: A General Concept for Flaw Identification Problems", *Mechanics Research Communications*, Vol. 20, p. 415-420.

Colaço, M.J., and Alves, C.J.S., 2013, "A Fast Non-Intrusive Method for Estimating Spatial Thermal Conductance by Means of the Reciprocity Functional Approach and the Method of Fundamental Solutions", *International Journal of Heat and Mass Transfer*, Vol. 60, p. 653-663.

Edmonds, M.J., Jones, A.M., O´Callaghan, P.W., and Probert, S.D., 1978, "The Prediction and Measurement of thermal Contact Resistance", *Wear*, Vol. 50, p. 299-319.

Fieberg, C., and Kneer, R., 2008, "Determination of Thermal Contact Resistance from Transient Temperature Measurements", *International Journal of Heat and Mass Transfer*, Vol. 51, p. 1017-1023.

Gill, J., Divo, E., and Kassab, A.J., 2009, "Estimating Thermal Contact Resistance Using Sensitivity Analysis and Regularization", *Engineering Analysis with Boundary Elements*, Vol. 33, p. 54-62.

Halliday, P.J., Parker, R., Piggott, R.B., Smith, A.C., and Steer, D.C., 1996, "Estimation of the Thermal Contact Resistance Between Potato Granules and Steel", *Journal of Food Engineering*, Vol. 28, p. 261-270.

Jiang, L., Wong, M., and Zohar, Y., 2001, "Forced Convection Boiling in a Microchannel Heat Sink", *Journal of Microelectromechanical Systems*, Vol. 10, p. 80-87.

ISSN 2176-5480

Kaipio, J. and Somersalo, E., 2004, "Statistical and Computational Inverse Problems", *Applied Mathematical Sciences* , Vol. 160, Springer-Verlag.

Krupadze, V., and Aleksidze, M. A., 1964, "The Method of Functional Equations for the Approximate Solution of Certain Boundary Value Problems", *Zh. Vychisl. Mat. Mat. Fiz.*, Vol. 4, p. 683-715.

Liu, J., Feng, H., Luo, X., Hu, R., and Liu, S., 2010, "A Simple Setup to Test Thermal Contact Resistance Between Interfaces of Two Contacted Solid Materiais", *11th International Conference on Electronic Packaging Technology & High Density Packaging*.

Luo, X., Feng, H., Liu, J., Liu, M.L., and Liu, S., 2011, An Experimental Investigation on Thermal Contact Resistance Across Metal Contact Interfaces", *12th International Conference on Electronic Packaging Technology & High Density Packaging*.

McWaid, T.H., and Marschall, E., 1992, "Application of the Modified Greenwood and Williamson Contact Model for the Prediction of Thermal Contact Resistance", *Wear* , Vol. 152, p. 263-277.

Milosevic, N.D., Raynaud, M., and Maglic, K.D., 2002, "Estimation of Thermal Contact Resistance Between the Materials of Double-Layer Sample Using the Laser Flash Method", *Inverse Problems in Engineering*, Vol. 10, p. 85-103.

Nissinen, A., Heikkinen, L., Kapio, J., 2008, "The Bayesian approximation error approach for electrical impedance tomography – experimental results", *Meas. Sci. Technol.*, Vol. 19, doi: 10.1088/0957-0233/19/1/015501.

Nissinen, A., Heikkinen, L., Kolehmainen, V., Kapio, J., 2009, "Compensation of errors due to the discretization, domain truncation and unknown contact impedances in electrical impedance tomography", *Meas. Sci. Technol.*, Vol. 20, doi: 10.1088/0957-0233/20/10/105504.

Nissinen, A., Kolehmainen, V., Kapio, J., 2011, "Compensation of modeling errors due to the unknown domain boundary in electrical impedance tomography", *IEEE Transactions on Medical Imaging*, Vol. 30 , p. 231–242.

Orlande, H. R. B., Dulikravich, G. S., Neumayer, M., Watzenig, D., and Colaço, M. J., 2013, "Accelerated Bayesian Inference for Estimating of Spatially Varying Heat Flux in a Heat Conduction Problem", *Numerical Heat Transfer - Part A - Applications*, (in press).

Tan, S., Fox, C., and Nicholls, G., 2006, *Inverse Problems, Course Notes for Physics 707*, University of Auckland.

Wolff, E.G., and Schneider, D.A., 1998, "Prediction of Thermal Contact Resistance Between Polished Surfaces", *International Journal of Heat and Mass Transfer*, Vol. 41, p. 3469-3482.

Yang, Y.-C., 2007, "Estimation of Thermal Contact Resistance and Thermally Induced Optical Effects in Single-Coated Optical Fibers", *Optics Communications*, Vol. 278, p. 81-89.

Zhang, X., Cong, P., Fujiwara, S., and Fujii, M., 2004, "A New Method for Numerical Simulation of Thermal Contact Resistance in Cylindrical Coordinates", *International Journal of Heat and Mass Transfer*, Vol. 47, p. 1091-1098.

9. RESPONSIBILITY NOTICE

The authors are the only responsible for the printed material included in this paper.